

CHARGE COLLECTION IN SIMPLE IPI DIODES

Larry D. Edmonds
(818) 354-2778, FAX (818) 393-4559

Jet Propulsion Laboratory¹
California Institute of Technology
Mail Stop 303-220
4800 Oak Grove Drive
Pasadena, California 91109-8099

ABSTRACT

Charge collection from ion tracks in epi diodes is investigated by computer simulations. As previously noted by others, collected charge can exceed charge liberated in the epi layer. Several cases are compared to illustrate the effects of changing ion LET, epi doping density, and doping types. It is found that the n^+-p - p^+ diode displays a funneling regime and a diffusion regime (as previously noted by others), but the p^+-n - n^+ diode does not. Simple models are proposed for quantitative estimates of collected charge. A qualitative two-state picture of funneling is discussed.

.....

1. The research described in this paper was carried out by the Jet Propulsion Laboratory, California Institute of Technology, under a contract with the National Aeronautics and Space Administration.

1. Introduction

Dodd et al. [1] and Dussault et al. [2] presented computer simulation results showing that charge collected in simple epi diodes can exceed the charge liberated by an ion in the epi layer (the Dussault paper also presents supporting experimental data). We have run our own simulations of this problem and our observations are consistent with some conclusions reached by Dodd et al. and Dussault et al. But a particular format for data presentation reveals additional conclusions that can be used to derive simple quantitative estimates of collected charge for a simple epi diode. The diode is "simple" in that there is only one upper junction, and a sharply defined doping profile distinguishes the epi layer from the substrate below. The doping is uniform in the epi layer and in the substrate.

An arbitrarily selected baseline case is the cylindrically symmetric problem shown in Figure 1. An ion track goes through an epi diode and charge collected by the single upper junction is investigated. Other cases are obtained by starting with the baseline case and changing each of several characteristics, one at a time. Each new case is compared to the baseline case. The baseline case is first compared to a bulk version of the Figure 1 problem. Then the effect of changing ion linear energy transfer (LET) is investigated. The effect of changing doping types is investigated next. Finally, the effect of changing the epi doping density is investigated.

As already pointed out by Dodd et al. [1], the n^+-p-p^+ diode shows a clearly defined funneling regime (early times) and diffusion regime (late times). But funneling (defined here as it was originally defined [3]) does not occur in the p^+-n-n^+ diode, although total collected charge can be nearly the same for the two cases.

A model is proposed for an upper bound estimate of charge collected during the funneling regime in the $n^+ \cdot p \cdot p^+$ diode. Another proposed model, applicable to both diode types, estimates total collected charge. Experimental data are consistent with the second model.

2. An Over-View of Charge-Collection Physics

It is interesting to compare the physics of charge collection in epi diodes to that in bulk diodes because there are as many similarities as differences. But discussion of these similarities requires some rather unconventional terminology. Instead of "funnels", emphasis is placed on voltages across several distinct device regions, where the regions themselves are defined by carrier densities. The discussion below begins with an attempt to discourage use of the conventional funnel terminology while simultaneously reviewing the sequence of events that led to the concept of a funnel. The discussion next introduces a more literal picture of funneling in terms of several interacting regions. Finally, the discussion points out similarities and differences between the bulk and epi cases. Bulk diodes are assumed until stated otherwise.

The 1981 Hsieh, Murley, and O'Brien paper [3] was the first on funneling and presented computer simulation results showing that an alpha particle track through a depletion region (DR) can cause the DR to collapse so that some or nearly all of the voltage normally across the DR is now across the substrate. They called this phenomena funneling. The paper introduced an "equivalent depth of collection" as a convenient measure of charge collected by funneling. The paper presented figures showing that there is an electric field throughout the entire device, but the field is weakest (equipotential surfaces are farthest apart) in the substrate near the DR, and much stronger near the bottom of the device. This is expected in view of the fact that the track

contributes to conductivity. Note that a weak electric field can produce a strong drift current in a highly-conductive track. Unfortunately, many investigators failed to notice this, and assumed that the substrate electric field was strongest near the DR. In fact, it was assumed that there exists a drift region adjacent to the DR having the property that the substrate electric field is essentially confined to within this region. By making the additional assumption that the drift-region depth is the same as the charge-collection depth, the picture of a funnel emerges. In this picture, a funnel is effectively an extension of the DR which contains a strong electric field that promptly collects all charge contained within.

The best-known paper that used this picture (in a time-average sense) for quantitative analysis is the 1982 McLean and Oldham paper [4]. The same authors later deduced that the physical picture is wrong for ions having a high LET and short range, because most of the substrate voltage drop is below the track. An empirical correction was made and presented in a 1986 paper [5]. The second paper pointed out that the original model is still valid (quantitative predictions agree with measurements) for alpha particles.

The success of the original model for alpha particles is, at least partly, a result of a cancellation of errors. One error is the assumption that the electric field is confined to a depth equal to the charge-collection depth. Another error is the failure to recognize that most charge collection occurs when the DR is partially recovered so that much of the device voltage is across the relatively narrow region occupied by a partially collapsed DR. Taken together, these errors over-estimate the time-average electric field strength in the substrate near the DR by an amount great enough to degrade the accuracy of any model, unless there are compensating errors. Some competing error is provided by the use of field-dependent mobilities. A more accurate field estimate will produce mobilities closer to the low-

field values than the values actually used. Another competing error is that diffusion currents are neglected, as implicitly implied when assuming that carriers move with a field-governed drift velocity. Diffusion is always important during funneling, as discussed later in this section. It is interesting that Hu [6] attempted a more careful analysis. Hu also neglected diffusion and assumed that carriers move with a drift velocity.¹ However, Hu recognized that the DR and a spreading resistance below the track each support some of the voltage. But by eliminating some compensating errors, Hu obtained a model that did not agree with experiment for n-type substrates [4].

Instead of looking for funnels, a more literal description of funneling is obtained by recognizing that the diode contains several distinct regions that interact with each other. By plotting electron and hole densities, together on the same graph, against a spatial coordinate, quasi-neutral regions are easily distinguished from space-charge regions. Such a plot clearly shows a reasonably well-defined boundary, the DR boundary (DRB), separating the DR from the quasi-neutral substrate. Funneling occurs when carriers generated in or near the DR are able to flood it so that it partially collapses.² A DR will be called partially collapsed when the voltage it supports is significantly less than it would be without the ion track. A partial collapse always implies a reduced DR width, but the converse is not necessarily true. A reduced width does not always imply collapse as defined here.

1. Another paper [7] compensated for this by adding twice the diffusion current to Hu's result, but recommended that the diffusion current be calculated from a linear diffusion equation with simple boundary conditions, which may not be good advice.

2. Carriers generated outside the DR can produce this state by diffusing in to produce flooding conditions. This was predicted theoretically under steady-state conditions [8] and verified by computer simulations for transient conditions.

So far there are two regions, consisting of the DR and quasi-neutral substrate. But the quasi-neutral substrate also divides into two regions. A theoretical steady-state analysis [8] predicted that a region would form, adjacent to the lower electrode, which is depleted of excess carriers and supports much of the substrate voltage. Because of a small conductance (compared to the high-density region above) and large voltage drop, this was called the high-resistance region (HRR). A strong electric field prevents minority carriers from entering this region and quasi-neutrality insures that there are essentially no excess majority carriers. The region is self-sustaining; the low conductivity results in a strong electric field that maintains the low conductivity. Computer simulations show a similar effect under transient conditions. In this case, the HRR is the region below the track (if the track is long enough to reach the lower electrode, the lower end will quickly clear away so that an HRR can form). Such a region is clearly visible in plots of potential, showing much of the substrate voltage to be across the low-conductivity region below the track, with a comparatively weak electric field along the track. Such a region can also be identified by plots of carrier density, showing an absence of downward diffusion.

The device voltage is divided between three regions (the DR, the HRR, and the quasi-neutral substrate section between them) and the amount of voltage across each region is governed by an interaction between the regions. Therefore the extent of DR collapse depends on global conditions and is not uniquely determined by carrier densities in the immediate vicinity of the DR.

The above statement is illustrated by computer simulation results comparing a bulk version of Figure 1 (same as Figure 1 except that the p^+ substrate is replaced by a continuation of the epi, and the "epi" is now called the "substrate") to an identical problem except that the ion track length was increased to 100 μm (the track reached the lower electrode). Simulations of the long-track case showed that the lower track end quickly cleared away

so, except during the very earliest times, it still makes sense to talk about an HRR below the track. But the HRR is very narrow for the long-track case and supports only a small voltage. Instead of a large voltage here, the DR quickly but partially recovered so that it supported a greater fraction of the device voltage. As expected, the long-track case produced a larger current during the short time prior to partial DR recovery. But after a very short time, the DR for the long-track case responded to global conditions (a small substrate resistance) by supporting more of the device voltage so that the currents for the two cases became nearly the same.

A more extreme case of a DR recovering in response to global conditions occurs when there is virtually no funneling at all. The McLean and Oldham model never questioned whether funneling actually occurs, i.e., whether a DR is significantly collapsed. Charge-collection depth was related to charge collected until the time at which the excess carrier density at the DRB drops down to the doping density, and the model simply assumes that funneling is full strength (all of the device voltage is across the charge-collection depth) during this time. It will be seen later that there are conditions such that the DR can support virtually all of the device voltage (no funneling) even when the carrier density at the DR boundary (DRB) greatly exceeds the doping density. The reason that some cases are more prone to funneling than others is easier to visualize from the qualitative discussion in Section 11. The most rigorous quantitative analysis (not a computer simulation) addressing this subject is presented in Reference [8], which solves nonlinear partial differential equations in three dimensions. The analysis applies to steady-state conditions, which can be obtained when photon irradiation replaces an ion track, but the steady-state problem has much in common with the transient problem. Many predictions from this analysis were verified by simulations for the transient problem.

It was stated earlier that diffusion is always important during

funneling and an explanation is now given. To the extent that the DRB can be approximated as stationary, it blocks the majority carrier current. When the DR is reverse-biased. This means that. majority carrier drift and diffusion currents have the same absolute values at the DRB. Under high-density conditions (defined by the carrier density greatly exceeding the doping density in the quasi-neutral region), the electron and hole densities are nearly equal in the quasi-neutral region, so the minority carrier drift and diffusion currents are also equal at the DRB (but they add instead of subtract.). The latter two currents are equally important and important.

Unfortunately, the conclusion that minority carrier drift approximately equals minority carrier diffusion under high-density conditions at the DRB does not imply that the minority carrier current is easy to calculate. The diffusion current is not necessarily the same as predicted by a linear diffusion equation. All cases define diffusion current to be proportional to the gradient of the carrier density function, but this gradient depends on whether the density function is governed by the linear diffusion equation or by a more complicated set of equations. However, when looking at a suitably restricted device region, we sometimes have the option of using a linear diffusion equation with modified boundary conditions as an approximate alternative to a more complicated equation with simple boundary conditions [8].

Epi diodes, like bulk diodes, can be partitioned into distinct regions, but there are four regions for the epi case. There is a DR, a quasi-neutral epi section, a space-charge region (denoted HI) associated with the epi/substrate high-low junction, and the quasi-neutral substrate below the HI. Computer simulation results show that the HI plays the same role in epi diodes as the HRR in bulk diodes. Most of the device voltage is usually shared by the DR and HI, with only a small voltage across the junction in the quasi-neutral epi region (and almost no voltage across the heavily-doped quasi-neutral substrate region). The potential profile

in an epi diode is qualitatively similar to that in a bulk diode, but with the HL substituting for the HRR. This produces some similarities in the charge-collection physics for the two cases.

An important difference between the epi and bulk cases is that the asymptotic value of collected charge, denoted $Q(\infty)$, is simple to calculate for the epi case, at least for the reverse-biasing conditions that have been considered. Agreement with computer simulation results is obtained by assuming that charge flow from the heavily-doped substrate to the epi is governed by minority carrier diffusion. But this is not enough to make $Q(\infty)$ simple. The simplifying observation is that the minority carrier density at the epi/substrate boundary is small compared to the density in the substrate interior, i. e., this boundary is sink-like for minority carriers. This uncouples interactions in the sense that minority carrier flow from the substrate to the epi is independent of conditions in the epi. Funneling influences the time profile of collected charge by influencing the rate that carriers in the epi are collected, but it does not affect the number of carriers that enter the epi from the substrate. This number is added to the number of carriers liberated in the epi to obtain $Q(\infty)$, and the result is valid with or without funneling.

The statements made in this overview are easier to visualize if illustrations are given. Sections 4 through 7 provide such illustrations. The charge-collection physics will be discussed again, but in more detail, in Sections 8, 9, and 11.

3. Carrier-Carrier Scattering

A theoretical analysis [9] concludes that a consistent treatment of carrier-carrier scattering (CCS) requires that the Einstein relation, relating diffusion coefficients to mobilities, be modified. The modified Einstein relation results in the ambipolar diffusion coefficient being unaffected by CCS. This conclusion

could be intuitively guessed if we think of ambipolar diffusion as a process in which electrons and holes move together. In reality, electrons and holes need not move together during ambipolar diffusion [8,10, Section 8 of this paper]. But they do in some special cases and that is good enough for this discussion. We could have guessed that CCS would not affect average carrier motion when both types of carriers are already thermalized and have the same average motion. To the extent that an ion track evolves via ambipolar diffusion, the time evolution of the track should not be affected by CCS. But failure to modify the Einstein relation can (depending on the CCS model) lead to extreme predictions, such as a track being "frozen" as if the carriers were immobile for an extended time. It may be better to not use CCS at all than to use it inconsistently.

The best approach for computer simulations is, of course, to include CCS consistently. It is speculated that the second-best approach, which should correctly predict track evolution, is to consistently neglect CCS, while the worst approach, which can predict frozen tracks, is to include CCS in some equations but not others. We are using an old version of PLSCES that follows the second-best approach.

4. Computer Simulations of the Baseline Case

The PLSCES prediction of collected charge for the Figure 1 arrangement is shown in Figure 2. The figure also shows collected charge for the bulk version, which is the same as Figure 1 except that the p^+ substrate is replaced by a continuation of the epilayer. The horizontal line is the charge liberated in the epi region. The epi version produces a larger current at early times, although total collected charge is reduced. However, the total collected charge does exceed the charge liberated in the epilayer. In this case the latter two charges differ by about a factor of 2, although this is not a universal number. Dussault et

al. [2] have found that total collected charge depends on substrate doping, and can range from one extreme (as much as the bulk device) to the other (charge liberated in the epi) .

The epi and bulk curves in Figure 2 are qualitatively similar to those in the corresponding figure presented by Dodd et al. [1]. As already pointed out by Dodd et al. , the corner in the epi device curve (0.9 ns in Figure 2 of this paper) is the transition between funneling and no funneling. This is the time at which the DR is completely recovered. A corresponding corner is not visible in the bulk device curve because DR recovery is much slower and the transition is more gradual. Two additional times, denoted t_1 and t_2 in Figure 2, were selected for a detailed look at conditions in the epi device.

Time t_1 (0.366 ns) is the time at which the epi and bulk devices in Figure 2 produce the same current. After this time the epi device produces the smaller current., and prior to this time. the epi device produces the larger current. This is also very close to the time at which the epi device collects an amount of charge equal to that liberated in the epi layer (it is not yet known whether or not this is an accident.) .

Several device regions at time t_1 are identified by electron and hole densities. Figure 3 plots these quantities as a function of distance on the axis of symmetry (the track) . For such large carrier densities in the lightly doped epi layer, quasi-neutrality is easily identified by the condition that the electron and hole densities are nearly equal. The figure shows a quasi-neutral section of the epilayer and a space charge region (the DR) , with the two regions separated by a reasonably well-defined boundary (the DRB) . On the other side of the quasi-neutral epi section is another space charge region associated with the high-low junction (HL) . The two regions are separated by another reasonably well-defined boundary (the first HL boundary or HLBI) . On the other side of the HL is another quasi-neutral region. In this heavily

doped region, quasi-neutrality is identified by the condition that the hole density is approximately the electron density plus the doping density. This region is separated from the HI₁ by the second HI₁ boundary HI₁B2. The terminology used in this paper regards the epilayer as the union of three regions: the DR (above the DRB), the quasi-neutral epi region (between the DRB and the HI₁B1), and the HI₁ (between the HI₁B1 and the HI₁B2).

The potential at time t_1 is plotted as a function of distance along the axis of symmetry in Figure 4. The figure also shows potential differences between various boundaries. The potential differences must add up to the applied voltage plus built-in potential, so the sum exceeds the applied 5 volts. It is seen that the DR supports less than half of the total voltage. The DR will be said to be partially "collapsed" when the supported voltage is significantly less than it would be without the ion track, so the figure shows a partially collapsed DR. Note that the DR width is also reduced. Figure 3 shows the width to be about $0.6 \mu\text{m}$. Without an ion track, the width would be about $3 \mu\text{m}$. If the strength of "funneling" is measured by the extent of DR collapse, then funneling is still strong at time t_1 even though the collected charge has already reached the value of the charge liberated in the epilayer. Figure 2 also suggests that funneling is still strong at this time. Note that there is very little voltage across the quasi-neutral epi region. However, even a weak electric field produces strong drift currents in a highly conducting track, and the current at time t_1 is large, as implied by Figure 2. As pointed out in Section 2, the potential profile shown in Figure 4 is qualitatively similar to that for bulk devices, but with the HI₁ substituting for the HRR.

Time t_2 (1.19 ns) is the time at which the current for the baseline problem is at a relative minimum. Charge collection is still occurring, but at a reduced rate. Carrier densities and potential are plotted in Figures 5 and 6. Most of the carriers have been removed from the epilayer. The DR has recovered and

supports nearly all of the device voltage. Funneling has stopped.

5. Computer Simulations of a Reduced LET Case

PL SCES was run again for a problem that is the same as Figure 1 except that the ion LET was changed from 40 to 1 MeV-cm²/mg. Collected charge is plotted as a function of time in Figure 7. For comparison purposes, the baseline case was normalized by dividing by 4 (I and plotted on the same graph). The low-LET curve shows a corner that is just as pronounced as that seen for the high-LET case. The collected charge up to this corner is by funneling, and exceeds the charge liberated in the epilayer, but only slightly. When comparing the high- and low-LET cases, we find that the asymptotic values of Q are nearly in the ratio of the LET's. But the low-LET case: results in a faster DR recovery, so this ratio is not observed at some definite but early time. For example, at 0.1 ns the ratio is about 24 instead of 40. Two additional times, denoted t_1 and t_2 in the figure, were selected for discussion.

Time t_1 (0.135 ns) is the time at which collected charge for the reduced LET case equals that liberated in the epilayer. Carrier densities and potentials are plotted in Figures 8 and 9. It is seen that the DR is partially collapsed and funneling is occurring. As with the high-LET case at the corresponding time, some of the epilayer voltage is across the HL. But, compared to the high-LET case, the low-LET case shows a much smaller conductance in the quasi-neutral portion of the epilayer, and this region supports a greater voltage and a greater fraction of the total epilayer voltage. Time t_2 (0.399 ns) is the time at which the current for the reduced LET case is at a relative minimum. It is not necessary to include detailed plots for this time point, because they merely confirm the expected result, that the DR is recovered and the population of electrons in the epilayer is much less than at time t_1 .

6. Computer Simulations of the p^+-n-n^+ Diode

PLSCEM was run again for a problem that is the same as Figure 1 except that p-types and n-types are interchanged and the polarity of the applied voltage is reversed. Collected charge is plotted as a function of time in Figure 10, which also shows the baseline case. The most noticeable characteristic of the new curve is that charge collection is at a reduced rate and there is no corner marking the end of the funneling regime. Even the amount of charge initially liberated in the DR ($3 \mu m$ worth of track length) is not "prompt" (an explanation is given in Section 8). The only way to determine the time at which the DR recovers is by looking at potential profiles at various times. Such an inspection has found that the DR recovery time is roughly 10 ps. Negligible charge collection has occurred up to this time, i.e., funneling plays no significant role, as discussed in more detail below.

For comparison purposes, time t_1 for the $p^{++}-n-n^+$ diode was selected to conform to t_1 for the baseline case. The nearest available time point is 0.377 ns. Carrier densities and potential at this time are plotted in Figures 11 and 12. The potential in Figure 12 is plotted with a reversed sign so that the figure will look more like previous figures. The HL is flooded so that width and voltage are negligibly small. Instead of two boundaries (n_1 and n_2), the HL region is represented by a single line in Figures 11 and 12. The DR supports nearly all of the device voltage at time t_1 , and at all times later than 10 ps, consistent with the assertion that funneling has no significant role.

Conditions resembling those shown in Figures 11 and 12 have been predicted theoretically. It is possible to predict a necessary condition, expressed in terms of the spatial distribution of carrier generation, for funneling to occur. If the condition is not satisfied, the DR will not collapse even when the carrier

density at the DRB greatly exceeds the doping density. Figures 11 and 12 illustrate a DR that has resisted collapsing under such conditions (they also show that a reduced DR width does not imply a collapse as defined in Section 2). It may be surprising that a DR can resist collapsing under high-density conditions, but this was theoretically predicted [8] before being observed in PLSCES results. The analysis also shows that the DR is most able to resist collapsing when the substrate is n-type. However, the analysis applies to steady-state conditions and a transient analysis remains to be worked out. If the steady-state analysis can be trusted for this transient prediction (this remains to be verified), funneling in p^+-n-n^+ ep diodes should be unimportant whenever the epi thickness is small enough so that ion IET is nearly uniform throughout the epilayer. Funneling might be important if the epi thickness significantly exceeds the track length.

7. Computer Simulations of an Increased Doping Case

Going back to the n^+-p-p^+ diode, PLSCES was run again for a problem that is the same as Figure 1 except that the epi doping density was changed from 8×10^{14} to 10^{16} cm^{-3} . Collected charge q is plotted as a function of time in Figure 13, which also shows the baseline case. Instead of showing a sharp corner, the new curve q is a compromise between the Figure 10 (no funneling) curve and the baseline (strong funneling) curve, suggesting that funneling is marginal for this case. This assertion can be verified by looking at conditions inside the device. Time t_1 was selected to conform to time t_1 for the baseline case. The nearest available time point is 0.363 ns. Carrier densities and potential at this time are plotted in Figures 14 and 15. The DR is nearly intact and supports nearly all of the voltage, indicating that funneling is very weak.

It might have been guessed that funneling would be weak for

this case, because the ratio of track density to doping density is reduced (compared to the baseline case) so nonlinear effects should be reduced. Although the guess agrees with PLSCS results, the reasoning behind the guess is wrong because the reduced LET case had an even smaller ratio of LET to doping density, but it still had a strong funneling regime. A better explanation is given in Section 11.

8. A High-Density Model for $Q(t_r)$

Let t_r denote the time of DR recovery, i.e., the time over which funneling occurs. Two values of collected charge that may be of interest are the value up to time t_r , $Q(t_r)$, and the total, $Q(\infty)$. This section treats the former value. This quantity is only meaningful for the $n^+ - p - p^+$ diode, so that is the case considered.

A model for calculating $Q(t_r)$ is easily derived from a number of approximations based on the assumptions suggested by Figure 3, of high-density conditions, i.e., the carrier densities in the quasi-neutral epi region greatly exceed the doping density until nearly all of $Q(t_r)$ has been collected. One requirement for the assumptions to be valid is that the ion LET be sufficiently large. The calculated value of $Q(t_r)$ will be found to exceed the charge liberated in the epi region, Q_{lib} . Therefore another necessary condition for the assumptions to be valid is that the track length and substrate diffusion length both be long enough so that the substrate can supply carriers to the epi region fast enough to maintain the assumed high-density conditions until nearly all of $Q(t_r)$ has been collected. The assumptions will obviously fail if the track length or substrate diffusion length are so short that the total charge available, $Q(\infty)$ (calculated in the next section), is less than $Q(t_r)$ calculated here. Expected deviations of actual collected charge from model predictions are discussed at the end of this section. For the time being, high-density conditions are taken for granted.

The assumed high-density conditions over the required time implicitly imply that the substrate is able to supply an adequate number of carriers to the epi region. This is all that needs to be said about the substrate. A complete set of equations for calculating $Q(t_r)$ can be derived by confining our attention to the quasi-neutral epi region, which is the region between the DRB and the HJBL. There are eight relevant current components: electron and hole, drift and diffusion, at two boundaries. These current components are shown in Figure 16. The subscripts have obvious interpretations. Arrows in the figure show the direction that each current refers to, and the directions are chosen so that each of the eight components is a positive quantity.

We start with the simplest equations. High-density conditions are assumed at the boundaries, as well as in the interior, so quasi-neutrality implies that the electron and hole densities are nearly equal and have nearly equal gradients at the boundaries. This means that electron and hole drift currents are in the ratio of the mobilities, and electron and hole diffusion currents are in the ratio of the mobilities. The first four equations are

$$J_{h,drift,D} = (\mu_h/\mu_e) J_{e,drift,D} \quad (1a)$$

$$J_{h,diff,D} = (\mu_h/\mu_e) J_{e,diff,D} \quad (1b)$$

$$J_{h,drift,H} = (\mu_h/\mu_e) J_{e,drift,H} \quad (1c)$$

$$J_{h,diff,H} = (\mu_h/\mu_e) J_{e,diff,H} \quad (1d)$$

The total current flowing into a quasi-neutral region equals the

total current flowing out, so another equation is

$$J_{e, \text{drift}, D} + J_{e, \text{diff}, D} + J_{h, \text{drift}, D} + J_{h, \text{diff}, D} =$$

$$J_{e, \text{drift}, H} + J_{e, \text{diff}, H} + J_{h, \text{drift}, H} + J_{h, \text{diff}, H} \quad (2)$$

A theoretical steady-state analysis [8] has shown that, for bulk devices under high-density conditions, there is an HRR (see Section 2) and another region above that is characterized by a large carrier density and weak electric field. It was shown that the carrier density is governed by the ambipolar diffusion equation in this region, hence the region was called the ambipolar region (AR). Figures 3 and 4 show similar regions, with the HL resembling the HRR and the quasi-neutral epi region resembling the AR. It is postulated that the carrier density in the quasi-neutral region is governed by the ambipolar diffusion equation. Note that this equation, which describes only the carrier density function and not carrier flow, does not imply that carrier motion is by diffusion. Different drift-assisted current densities can be compatible with the same carrier density function if the currents have the same divergences (a 7% divergence means that carriers leaving a volume element are replaced by others moving in). Therefore, by postulating the ambipolar diffusion equation in the quasi-neutral region, we are not ruling out drift currents. Even weak electric fields produce strong drift currents in high-density tracks. Also note that a linear diffusion equation is postulated for the carrier density (not carrier flow) even though earlier discussion (Section 2) stated that this may not be appropriate. The catch, for bulk devices under steady-state conditions, is that the equation can only be used if boundary conditions are modified to account for HRR width. This is an alternative (as pointed out in Section 2) to a nonlinear equation with simpler boundary conditions. Epi devices are simpler because the HLB is always at nearly the same location. But we should

assume carrier-density boundary conditions shown in Figure 3 as opposed to Figure 11.

The above postulate makes the carrier density gradients (and diffusion currents) solvable, except for one complication. The DRB is moving. From the point of view of minority carriers, the DRB resembles a vacuum cleaner moving down (to the right in Figure 16). A moving vacuum cleaner collects more carriers than a stationary vacuum cleaner. This is consistent with Figure 3, which implies a larger gradient near the DRB than at the HIB1 (logarithmic scales obscure visual impression of slopes, but the slopes do compare as stated). From the point of view of majority carriers, the DRB is a barrier that pushes them along in front of it as it moves. This produces a majority carrier current at the DRB. DRB motion also affects the relationship between electron current surface integrals and the rate of change of the number of electrons contained in a volume. There can be a rate of change without any current if the volume changes. If we neglect the influence of DRB motion on currents, we obtain one error. If we neglect the influence of DRB motion on the conservation equation, we obtain a second error. It can be shown that the two errors partially (not completely) cancel, suggesting that we may obtain an adequate approximation by pretending that the DRB is stationary.

A geometric simplification is to assume that the track hits near the center of the DR and that the DR lateral dimensions are at least as large as the epilayer thickness. This makes the diffusion problem quasi-one-dimensional (variations with lateral coordinates can be eliminated by integrating with respect to the lateral coordinates). The carrier densities at the DRB and HIB1 are assumed greater than the doping density but, as suggested by Figure 3, still small compared to the density in the quasi-neutral epilayer interior. For the purpose of calculating gradients from the diffusion equation, both boundaries can be regarded as

sinks.¹ With the DRB assumed stationary, the symmetry of the boundary value problem implies that

$$J_{e, \text{diff}, D} = J_{e, \text{diff}, H}. \quad (3)$$

Note that we could go a step further and use the ambipolar diffusion equation to explicitly evaluate the time integral of each side of (3). But, the resulting equation will be a linear combination of the equations already listed and those still to come.

A stationary DRB also blocks the hole current, so another equation is

$$J_{h, \text{drift}, D} = J_{h, \text{diff}, D}. \quad (4)$$

The final equation is conservation of electrons. Ignoring recombination in the epi region, the time integral of the electron current at the DRB minus that at the HLB is equated to the change in the number of electrons in the quasi-neutral epi region. The final number is negligible compared to the initial number, so the change in the number of electrons is simply the initial number. But it may not be obvious what the initial number is, because the track liberates carriers not only in the quasi-neutral epi region, but also in the DR and HL. It is convenient to visualize the track as being created instantaneously. We can let $t=0$ refer to any convenient time after the track formation,

1. This illustrates the fact that the ambipolar diffusion equation describes only the carrier density function, not carrier flow. Electron flow at the HLB is directed into the quasi-neutral epi region, not out. The HLB is not a sink for electrons, it is a source. It can be regarded as a sink only for the purpose of calculating carrier density gradients from the diffusion equation.

providing that there is negligible charge collection at the device terminals up to this time. To avoid the necessity of considering a rapidly moving DRB (if the DRB is even defined during DR collapse), it is convenient to let $t=0$ be the end of the collapse stage and the beginning of the recovery stage. Let $t=0^-$ refer to the time of track formation, before the DR has collapsed. At this time the DR is the same region as the pre-ion-hit DR. The track is electrically neutral (an equal number of electrons and holes) and the carriers have not yet had time to move. Following this state is a rearrangement of carriers (a charge separation) resulting in some of the previously unshielded impurity ions becoming shielded, and the DR collapses.¹ During the collapse, the DRB moves up (at least conceptually, it might not be defined during this time) while holes are simultaneously pushed down below the DRB. All holes initially liberated in the pre-ion-hit DR end up in the (now larger) $t=0$ quasi-neutral epi region. Quasi-neutrality insures that this supply of holes is accompanied by a nearly equal number of electrons. As far as the number of electrons in the $t=0$ epi region is concerned, the end result is the same as if the DRB moved up, leaving all carriers in the pre-ion-hit DR behind so that they now find themselves in the quasi-neutral epi region. When there is a nearly complete DR collapse, there is no sharp distinction between carriers liberated in the DR and those liberated in the $t=0^-$ quasi-neutral epi region, both groups end up in the $t=0$ quasi-neutral epi region.² This statement is consistent with all figures showing $Q(t)$. The amount of charge liberated in the DR has no special significance

1. Computer simulations show a very fast current "bump" that might be associated with this charge rearrangement (possibly a Capacitance effect,). But this current bump has not yet been found to significantly contribute to collected charge. Most charge collection occurs during the recovery stage.

2. There is not even a sharp distinction in terms of collapsing the DR. Carriers liberated outside of the DR can diffuse in and produce a collapse. This was predicted theoretically for steady-state conditions [9] and verified by PISCES for transient conditions.

in any of the curves.

Now consider carriers liberated in the HI. The collapsing DR results in a voltage across the HI that adds to the built-in potential. The result is a strong electric field in the HI that will drive electrons into the quasi-neutral epi region until the carrier density gradient in the HI is large enough for the diffusion current to nearly balance the drift current. As soon as this near-balance occurs, the number of electrons in the HI is much less than the $t=0$ value, nearly all have moved into the quasi-neutral epi region.

We conclude from the above discussion that the number of electrons in the $t=0$ quasi-neutral epi region is simply Q_{lib}/q , the number liberated above the HIB2. Let Q with a subscript be the time integral (from 0 to t_r) of the current having the same subscript. The final equation is

$$Q_{e,drift,D} + Q_{e,diff,D} - Q_{e,drift,H} + Q_{e,diff,H} = Q_{lib} \quad (5)$$

Using

$$Q(t_r) = Q_{e,drift,D} + Q_{e,diff,D} \quad (6)$$

and solving the simultaneous equations consisting of (5), (6), and the time integrals of (1) through (4) gives

$$Q(t_r) = (1/2) (1 + \mu_e/\mu_h) Q_{lib} \quad (7)$$

A number of assumptions were used to derive (7). The geometric

assumptions (a centered junction at a junction with lateral dimensions at least as large as the epi thickness) implying a quasi-one-dimensional problem are still assumed, but we now consider what may happen when some of the other assumptions fail. One of the assumptions was that the substrate can supply carriers to the epi region in sufficient quantity to maintain high-density conditions until the model predicted $Q(t_r)$ has been collected. This assumption clearly fails if the track length and/or substrate diffusion length are so short that $Q(\infty)$ (calculated in the next section) is less than $Q(t_r)$ calculated from (7). The actual $Q(t_r)$ must be less than calculated from (7).

Another way for the assumptions to fail is for the ion LET to be too small. If we look at the low-LET case shown in Figure 8, we find that the equation that is most visibly wrong is (1c). The electron and hole densities are not nearly equal at the HBB, so the drift currents are not in the ratio of the mobilities. The proper ratio of drift currents contains another factor, which is the ratio of the hole density to the electron density. If we set a fudge factor f equal to some kind of time and radial average of the latter ratio, (1c) is replaced with

$$J_{h, \text{drift}, H} = (\mu_h / \mu_e) \cdot J_{e, \text{drift}, H} \quad (8)$$

and repeating the previous analysis gives

$$Q(t_r) = 2[(f + \mu_e / \mu_h) / (1 + 3f)] Q_{\text{lib}} \quad (9)$$

The value of f at the particular time and radial coordinate represented in Figure 8 is about 1.7. It is not obvious what value represents a time and radial average, but the value 2.6 produces agreement with the collected charge shown in Figure 7.

It should be noted that the high-density model is an idealization that even an I_{HI} of 40 does not produce. The same considerations just discussed for the low-LET case also apply to higher LETs, but, to a lesser extent. Figure 3 suggests that the approximations should be good, but this figure refers to a radial coordinate of zero, where the carrier density is greatest. At larger radial coordinates, the ratio of hole to electron drift currents at the HLB1 will differ from the ratio of mobilities. Because of a large HLB1 area, the contribution to surface integrated hole drift current from the larger radial distances is not negligible. In general, the model prediction is expected to be an upper bound for the actual $Q(t_r)$. This upper bound is most closely approached by high-LET ions having a long range in a substrate having a relatively long lifetime. Deviations from these conditions tend to reduce the actual $Q(t_r)$. Model accuracy could be improved by using an empirical fudge factor f in (9). Values of f that fit some data (see Section 14) range from 1.5 to 2.6.

It should be pointed out that the predicted $Q(t_r)$ scales with ion LET, but even if the model was equally accurate for any LET, this would still not imply that collected charge up to a given time t scales with LET. When comparing $Q(t_r)$ for different cases, we are comparing Q at corresponding times but different times. Charge collection can be faster for one case than for another.

9. A Model for $Q(\infty)$

Unlike the high-density model for $Q(t_r)$, the proposed model for $Q(\infty)$ appears (judging from several PLSCS examples) to be accurate and applicable to all cases, including the $p-n^+n^+$ diode. No fudge factors are needed to improve accuracy. The proposed model is obvious; we add to Q_{jib} the charge that diffuses from the s_{ii} to the epi layer. But the diffusion current depends on boundary conditions at the HLB2, so it is still true to look at

the PLSCES predicted carrier densities shown in Figure 3. This is the baseline case prior to DR recovery. The electron density in the substrate at this time is almost as large as the doping density, and will be even larger at earlier times. Use of the minority carrier diffusion equation to describe carrier densities and electron diffusion current may seem questionable. But the figure refers to a zero radial coordinate where the carrier density is greatest. At larger radial distances and/or at later times, the minority carrier diffusion equation will clearly apply to this example.

Given that the minority carrier current from the substrate to the epi region is diffusion, as predicted by the minority carrier diffusion equation, the important observation from Figures 3, 5, 8, 11, and 14 is that the HLB2 is a sink-like boundary for minority carriers. This means that the diffusion current does not depend on conditions inside the epi layer, and is therefore easy to calculate under simple geometric conditions. If the ion LET is nearly uniform and if the track length in the substrate, as well as all substrate dimensions, is much greater than the substrate diffusion length, the number of minority carriers that diffuse to the sink-like boundary HLB2 is simply the number liberated within a minority carrier diffusion length from this boundary. Therefore $Q(\infty)$ is estimated, for these simple geometric conditions, to be the charge liberated in the region that includes the epi layer and extends an additional diffusion length below the epi layer.

For the more general case of a nonuniform LET and/or a short track, we can numerically integrate contributions from track sections, or find analytic fits to LET or range data so that the integral can be evaluated analytically. Either way, we need to know the amount of charge that diffuses to the epilayer, δQ_{diff} , when some amount of charge, δQ , is liberated a perpendicular distance y below the epi layer. A simple diffusion analysis, applicable when the substrate diffusion length, L_D , is small compared to all substrate dimensions, concludes that the equation

is

$$\delta Q_{diff} = \exp(-y/l_D) \delta Q . \quad (10)$$

10. Comparison Between Model Predictions and PISCES Results

When comparing model predictions to PISCES results, we should, for internal consistency, use the same mobilities and lifetimes that PISCES used. It is possible to make PISCES print out these quantities, and it was found that the electron and hole mobilities in the epilayer for the baseline problem were 1310 and 495 cm²/V-sec, respectively. The value of $Q(t_r)$, without the fudge factor, is calculated from (9) to be about 1.8 times Q_{jib} . This should be an upper bound for the actual $Q(t_r)$ and should apply to both the baseline case and the reduced LET case. The value of $Q(t_r)$ calculated from PISCES is found from Figures 2 and 7 to be about 1.3 and 1.2 times Q_{jib} for the baseline and reduced LET cases, respectively. As expected, the baseline case comes closer to the model prediction. The values for the fudge factor f needed to make (9) agree with PISCES are 2.1 and 2.6 for the baseline and reduced LET cases respectively.

For the increased doping case, the electron and hole mobilities in the epilayer were: 1076 and 461 cm²/V-sec, respectively. The calculated value of $Q(t_r)$, without the fudge factor, is about 1.67 times Q_{jib} . The value calculated by PISCES appears, from Figure 13, to be about 1.25 times Q_{jib} . The value of f needed to produce agreement is about 1.95.

It is interesting that data presented by Dodd et al. [1] are consistent with our own PISCES predictions, although it is not clear what the mobilities were because CCS models were used. Referring to Figure 5 of the Dodd paper, $Q(t_r)$ appears to be about 1.1 pC. This was produced by a 100 MeV Fe ion (LET=29) in a

2.5 μm epi layer, so $Q_{jib} = 0.5 \text{ pC}$ and $Q(t_r)$ is about 1.5 times Q_{jib} . If we pretend that the mobilities are in the same ratio as those used in our own simulations for the baseline case, we find that the value of f needed to produce agreement is 1.5.

To estimate $Q(\infty)$, we need the minority carrier diffusion length in the substrate. The electron and hole mobilities used by PISCES in the substrate were 252 and 178 $\text{cm}^2/\text{V}\cdot\text{sec}$, respectively. Based on arbitrary data that we supplied, PISCES calculated the lifetime in the substrate to be 400 ns. This produces a minority carrier diffusion length of 5.6 μm for all n^+p diode cases. Adding this to the 5 μm epi thickness, the estimated values of $Q(\infty)$ are 2.12 times Q_{jib} for all such cases. For the p^+n diode, $Q(\infty)$ is estimated to be 1.94 times Q_{jib} . Comparing these predictions to Figures 2, 7, 10, and 13 shows reasonably good agreement for all cases.

11. A Two-State Picture of Funneling

It was found that, even under high-density conditions, funneling sometimes occurs and sometimes does not. It is reasonable to ask why there are two possibilities. This question was quantitatively answered for bulk diodes under steady-state conditions [8], but mathematical complexity obscures physical understanding. An intuitive picture can be obtained by ignoring the fact that there are different degrees of DR collapse and pretending that only two states are possible: funneling and no-funneling. The DR is either completely collapsed or completely intact. The epi diode appears to be qualitatively similar to the bulk diode, with the HJ in the epi diode substituting for the HRR in the bulk diode. The bulk case is discussed because conclusions are supported by quantitative analyses.

First consider the HRR, which is a region adjacent to the lower electrode. In reality, the HRR always has a small conductivity

(compared to the region above it under high-density Conditions) but it can have various widths and support various voltages. But in this two-state picture we will visualize the HRR as a fixed region which can have different conductivities. The most obvious state possible for the HRR if the track is long enough to come near it is to be flooded with carriers, i.e., it is shorted and supports no voltage. But another state is also possible, Given that there is (somehow) a large voltage across the HRR, a strong electric field prevents minority carriers from entering and drives out those already present. Quasi-neutrality insures that there are essentially no excess majority carriers, so the conductivity is low. This is a self-sustaining state. A strong electric field maintains a low conductivity which maintains a strong electric field.

Similarly, one state possible for the DR is to be flooded (shorted), but another possible state has a strong electric field that sweeps out carriers and keeps the density below flooding levels. When the DR and HRR are in series, they can both be shorted momentarily but, in the absence of a current limiting external resistance, they cannot both remain in shorted states (the region separating them supports little voltage). Only one can remain in a shorted state and the other is forced into a voltage-supporting state. If the DR is shorted we have funneling, if the HRR is shorted we do not.

One obvious conclusion from the above discussion is that the occurrence of funneling depends on the location and length of the ion track. If a high-density track is localized near the DR, the DR will have the stronger tendency to short and funneling occurs. If the track is localized near the HRR (this is possible if the track is produced by a proton-induced nuclear reaction product), the HRR has the stronger tendency to short and funneling does not occur.

This picture, combined with some additional information, can

explain why funneling is so marginal for the increased doping case shown in Figures 13, 14, and 15. As already noted, the explanation is not simply that there is a reduced ratio of track density to doping density, because an even smaller ratio produced strong funneling for the reduced LET case. The proper explanation involves a property of the DR. Under low-density conditions, the DR is characterized by a near balance between drift and diffusion currents. In fact, equating total electron and hole currents to zero is a simple way to derive the classical law of the junction, which relates carrier density to potential. In order to flood or collapse a DR, it is necessary for total minority carrier current to be nonnegligible compared to the individual drift and diffusion components. Increased doping produces increased drift and diffusion currents, so the current required to collapse the DR increases. The DR becomes more difficult to short while the HRR (or HR for epi diodes) becomes easier to short. The relative ease of shorting the two regions shifts with increased doping. Hence, funneling is more difficult to induce when the doping is increased, even if ion LET is increased by the same ratio.

Although not intuitively obvious (there is a mathematical explanation [8]), the HRR has a stronger tendency to short when the substrate is n-type than for the p-type case, even when doping densities are selected so that both types have the same conductivities. Compared to the p-type case, funneling for the n-type case requires carrier generation to be closer to the DR. If carriers are generated under steady-state conditions, funneling does not occur in the n-type substrate when the generation is spatially uniform throughout the diode, but can occur for the p-type case. PLSCES results show that, for epi diodes under transient conditions, funneling does not occur in the n-type diode when the track is uniform in the epilayer, but can occur for the p-type diode.

12. Experimental Data

Techniques pioneered by McNulty et al. [11] were used to measure collected charge from an n-type substrate epi CMOS SRAM, from alpha particles having several energies. A charge-sensing preamplifier was connected to the device supply line and a histogram of the resulting pulse distribution was collected by a multi-channel analyzer (MCA). By monitoring the sum of currents from all nodes, the device simulates a large-area diode. The time scale used for the measurements was too long to reach any conclusions regarding $Q(t_p)$, but $Q(\infty)$ was measured. Collected charge measurements were taken from MCA peak centers and calibrated using a surface barrier detector. The 2 MeV alpha particles resulted in broad peaks due to variations in overlayer stopping thickness. Peak centers were determined by center-of-mass type calculations. The peaks are much sharper for higher energies.

The device had a grown epi thickness of $9\text{ }\mu\text{m}$, which should reduce to about $5\text{ }\mu\text{m}$ after processing [12]. Overlayer thickness and substrate diffusion length are unknown but can be inferred from the data. Overlayer thickness is relevant (at low energies) because it affects σ_{eff} and penetration depth below the overlayer. Estimates of the various thicknesses are those values that make the model-predicted $Q(\infty)$ agree with measurements. Model predictions were calculated by first using TRIM to calculate alpha particle energy versus travel distance in silicon. These data easily calculate Q_{epi} when overlayer thickness, epi thickness, and initial alpha particle energy are assumed. For ion tracks long enough to go through the epi, charge diffusing to the epi, Q_{diff} , must also be calculated. A numerical integration sums contributions from many small track sections, with TRIM results used to calculate δQ for each section and (10) used to calculate δQ_{diff} .

Very good agreement between model predictions and measurement was obtained using a $4\text{ }\mu\text{m}$ average overlayer thickness, a $5\text{ }\mu\text{m}$ epi

thickness, and an $11.5 \mu\text{m}$ substrate diffusion length. Note that overlayer thickness includes all dead layers and is a silicon equivalent, which will be larger than actual physical dimensions if there are any very dense structures. Furthermore, the device was planarized, which also tends to increase overlayer thickness. Therefore, the $4 \mu\text{m}$ estimate is credible. A comparison between model predictions and measurement is shown in Figure 17. The very good agreement using the expected epi thickness tends to validate the model. Other epi thicknesses cannot produce such good agreement., no matter how the other parameters are selected.

Additional validation was obtained from a second device, identical to the first except that a very large fluence from very heavy ions (a result of many latchup tests) degraded the substrate lifetime. Using the same overlayer and epi thickness used for the first device, but selecting substrate diffusion length to fit the data ($2.5 \mu\text{m}$), produced the comparison shown in Figure 18. The charge collection depth is small for this device, hence it collects much less charge at the higher energies than the first device. Collected charge for the second device decreases with increasing energy above 3 MeV because track length is longer than the charge collection depth and ion LET decreases with increasing energy. A less-than-perfect fit between model predictions and measurement is attributed to a small recombination loss in the epi layer. The fit is good enough to add additional credibility to the model.

13. Conclusion

A proposed upper bound for $Q(t_p)$ is the value calculated from (7). The modified equation (9) would give a more accurate estimate, except that f is unknown. From a practical point of view, the modified equation is useless if we have no idea of what the numerical value of f is. From an academic point of view, the equation is informative because we know what f represents. It is

an average ratio of hole density to electron density at the HLB1. We also know the conditions that tend to make f increase or decrease. It decreases and approaches 1 in the high-density limit. We can also see from (9) how f influences $Q(t_r)$. Compared to a low-IET ion, a high-IET ion produces a smaller f and the actual $Q(t_r)$ is more nearly equal to the upper bound calculated from (7). However, even a very high-IET ion cannot sustain conditions resembling the high-density limit for the required time if the track length in the substrate and/or substrate diffusion length are negligibly small. In this case, the actual $Q(t_r)$ cannot exceed Q_{ib} .

The time dependence of charge collection is influenced by funneling and changes when conditions change, but the total amount collected, $Q(\infty)$, is simple and calculated the same way for all cases. Judging by several PISCES examples, a reasonably accurate estimate is obtained by adding to Q_{ib} the amount of charge that diffuses from the substrate to the epilayer. Experimental data are consistent with this model. From a practical point of view, it is unlikely that we will have an accurate estimate of the substrate diffusion length in a real device unless collected charge is measured, so estimates of $Q(\infty)$ will be uncertain. From an academic point of view, the simplicity of the model is very appealing.

Collected charges were compared for several changes in conditions. A comparison between different ion LETs when all other conditions are the same is shown in Figure 7. The asymptotic values of Q are nearly in the ratio of the LETs. But the low-LET case produces a faster DR recovery. Therefore, when comparing collected charges at the same (not corresponding) and early time, this ratio is not observed. For example, Figure 7 shows a ratio at 0.1 ns of 24 instead of 40.

The effects of increased epi doping is shown in Figure 13. Only marginal funneling occurred for this case. The comparison that

may be the most interesting is shown in Figure 10, which compares the two diode types. The values of $Q(\infty)$ are comparable, but the p^+-n-n^+ diode does not show a funneling regime, and charge collection at early times is at a reduced rate compared to the other case. It was found that the DR was able to resist collapsing even though the carrier density at the DRB greatly exceeded the doping density. This observation is consistent with quantitative theoretical predictions. A two-state picture makes qualitative cause/effect relationships easier to visualize.

REFERENCES

- [1] P.E. Dodd, F.W. Sexton, and P.S. Winokur, "Three-Dimensional Simulation of Charge Collection and Multiple-Bit Upset in Si Devices, " IEEE Transactions on Nuclear Science, vol.41, no. 6, pp.2005-2017, December 1994.
- [2] H. Dussault, J.W. Howard Jr. , R.C. Block, M.R. Pinto, W.J. Stapor, and A.R. Knudson, "High Energy Heavy-Ion-Induced Single Event Transients in Epitaxial Structures, " IEEE Transactions on Nuclear Science, vol.41, no.6, pp. 2018-2025, December 1994.
- [3] C.M. Hsieh, P. C. Murley, and R.R. O'Brien, "A Field-funneling Effect on the Collection of Alpha-Particle-Generated Carriers in Silicon Devices, " IEEE Electron Device Letters, vol. EDL-2, no. 4, pp. 103-105, April 1981.
- [4] F.B. McLean and T.R. Oldham, "Charge Funneling in n- and p-Type Si Substrates, " IEEE Transactions on Nuclear Science, vol. NS-29, no.6, pp.2018-2023, December 1982.
- [5] T. R. Oldham, F.B. McLean, and J.M. Hartman, " Revised Funnel Calculations for Heavy Particles with High dE/dx, " IEEE Transactions on Nuclear Science, vol. NS - 33, no. 6, pp. 1646-1650, December 1986.
- [6] C. Hu, "Alpha-Particle-Induced Field and Enhanced Collection of carriers, " IEEE Electron Device Letters, vol. EDL-3, no. 2, pp. 31-34, February 1982.
- [7] L. D. Edmonds, "A Simple Estimate of Funneling-Assisted Charge Collection, " IEEE Transactions on Nuclear Science, vol. 38, no.2, pp. 828-833, April 1991.
- [8] L. Edmonds, "A Theoretical Analysis of Steady-State Photocurrents in Simple Silicon Diodes, " Jet Propulsion Laboratory Publication 95-10, March 1995.
- [9] T.T. Mamatkhanov, I.I. Rostovtsev, and N.I. Philatov, "Investigation of the Effect of Nonlinear Physical Phenomena on Charge Carrier Transport in Semiconductor Devices, " Solid-State Electronics, vol. 30, no.6, pp. 579-585, 1987.
- [10] Oldwig Von Roos, "A Note on Photocurrents in Extrinsic Semiconductors, " Solid-State Electronics, vol.22, pp.229-232, 1979.
- [11] P.J. McNulty, W. J. Beavens, and D. R. Roth, "Determination of SEU Parameters of NMOS and CMOS SRAMS, " IEEE Transactions on Nuclear Science, vol. 38, no. 6, pp. 1463-1470, December 1991.
- [12] D. Takacs, J. Harter, E.P. Jacobs, C. Werner, U. Schwabe, J. Winnerl, and E. Lange, "Comparison of Latch-Up in P- and N-Well CMOS Circuits, " IEEE Nuclear Science Digest, pp. 159-163, 1983.

FIGURE CAPTIONS

Figure 3: The diode and ion track defining the baseline problem (not drawn to scale).

Figure 2: Collected charge as a function of time for the baseline problem and for a bulk version of the problem. The horizontal line is the charge liberated in the epilayer.

Figure 3: Electron and hole densities for the baseline problem at time t_1 shown in Figure 2.

Figure 4: Potential for the baseline problem at time t_1 shown in Figure 2.

Figure 5: Electron and hole densities for the baseline problem at time t_2 shown in Figure 2.

Figure 6: Potential for the baseline problem at time t_2 shown in Figure 2. Off-scale arrow indicates that the first potential difference is across the entire DR.

Figure 7: Collected charge as a function of time for the reduced LET problem. Also shown is the normalized (divided by 40) curve for the baseline case. The horizontal line is the charge liberated in the epi layer.

Figure 8: Electron and hole densities for the reduced LET problem at time t_1 shown in Figure 7.

Figure 9: Potential for the reduced LET problem at time t_1 shown in Figure 7. Off-scale arrow indicates that the first potential difference is across the entire DR.

Figure 10: Collected charge as a function of time for the p^+-n-n^+ diode. Also shown is the curve for the baseline case. The horizontal line is the charge liberated in the epi layer.

Figure 11: Electron and hole densities for the p^+-n-n^+ diode at time t_1 shown in Figure 10.

Figure 12: Potential (with reversed sign) for the p^+-n-n^+ diode at time t_1 shown in Figure 10.

Figure 13: Collected charge as a function of time for the increased epi doping problem. Also shown is the curve for the baseline case. The horizontal line is the charge liberated in the epi layer.

Figure 14: Electron and hole densities for the increased epi doping problem at time t_1 shown in Figure 13.

Figure 15: Potential for the increased epi doping problem at time t_1 shown in Figure 13.

Figure 16: The eight current components at the two quasi-neutral epi region boundaries. Arrows indicate directions that make all components positive for n^+-p-p^+ diodes.

Figure 17: Comparison between predicted and measured Q for an epi SRAM.

Figure 18: Same as Figure 17 except that the SRAM has a degraded substrate lifetime.

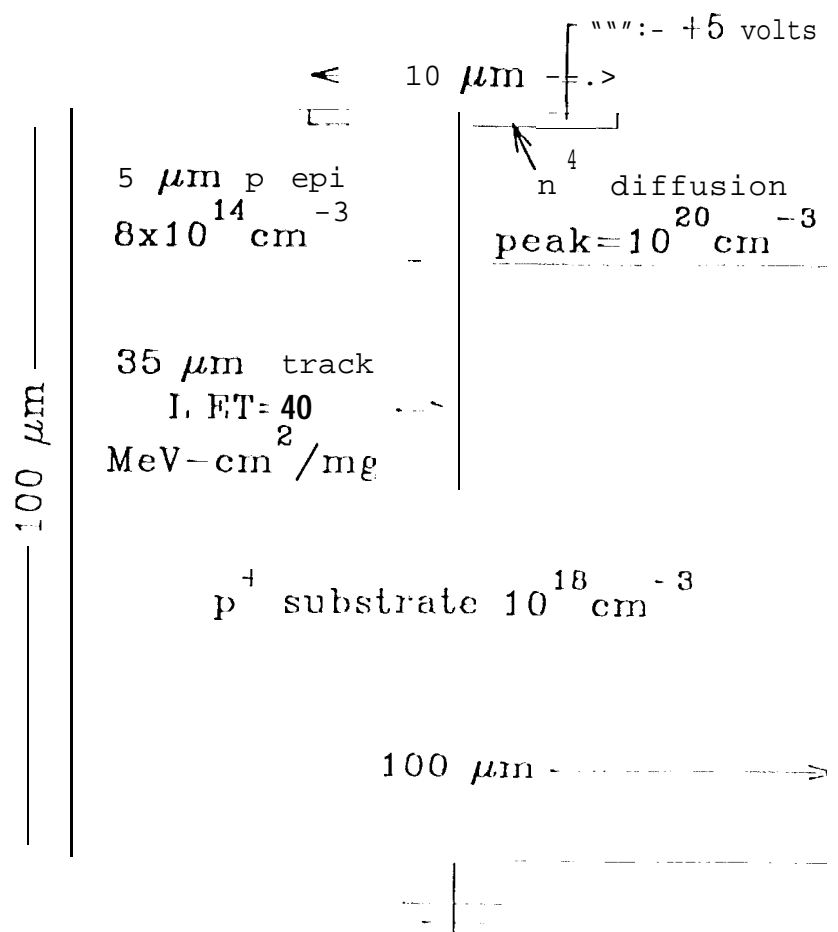


Figure 1: The diode and ion track defining the baseline problem (not drawn to scale).

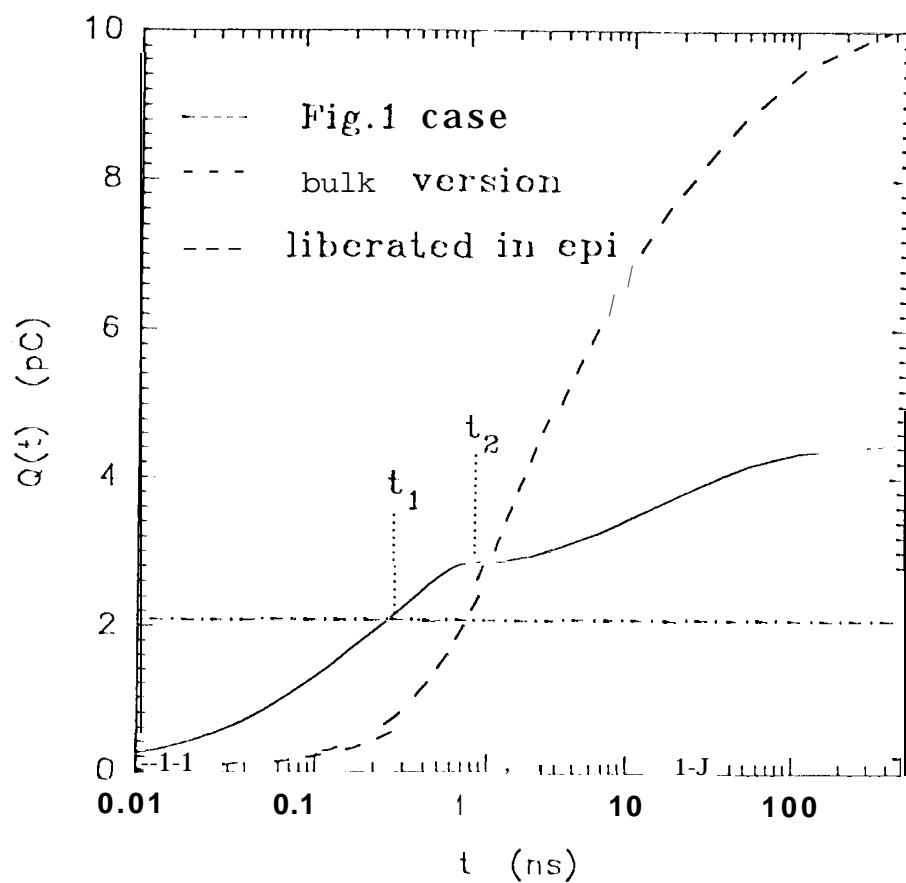


Figure 2: Collected charge as a function of time for the baseline problem and for a bulk version of the problem. The horizontal line is the charge liberated in the epi layer.

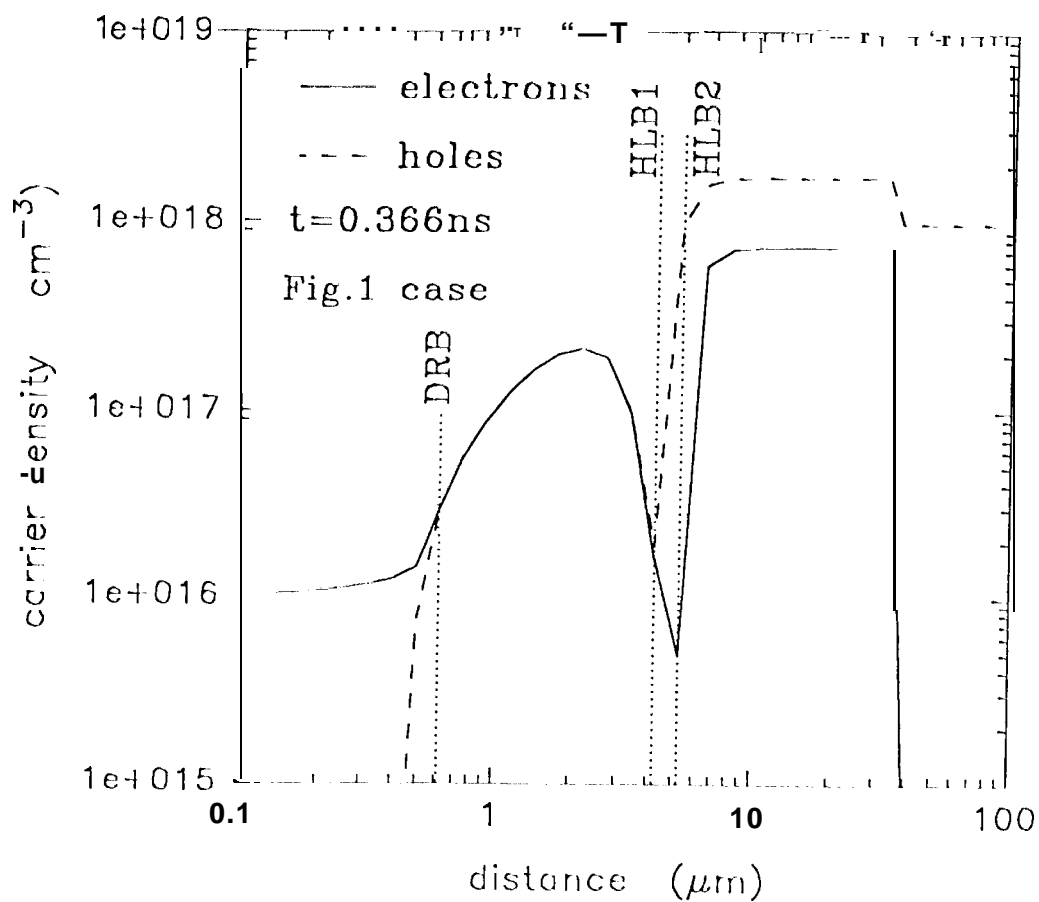


Figure 3: Electron and hole densities for the baseline problem at time t_1 shown in Figure 2.

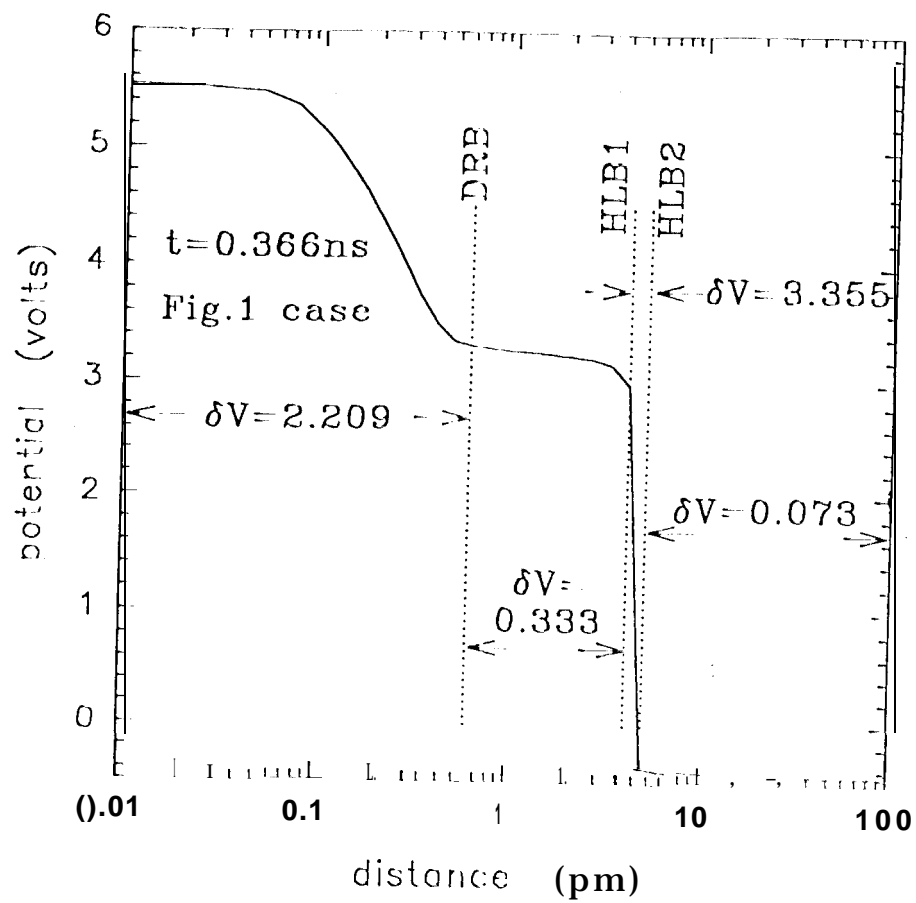


Figure 4: Potential for the baseline problem at time t_1 shown in Figure 2.

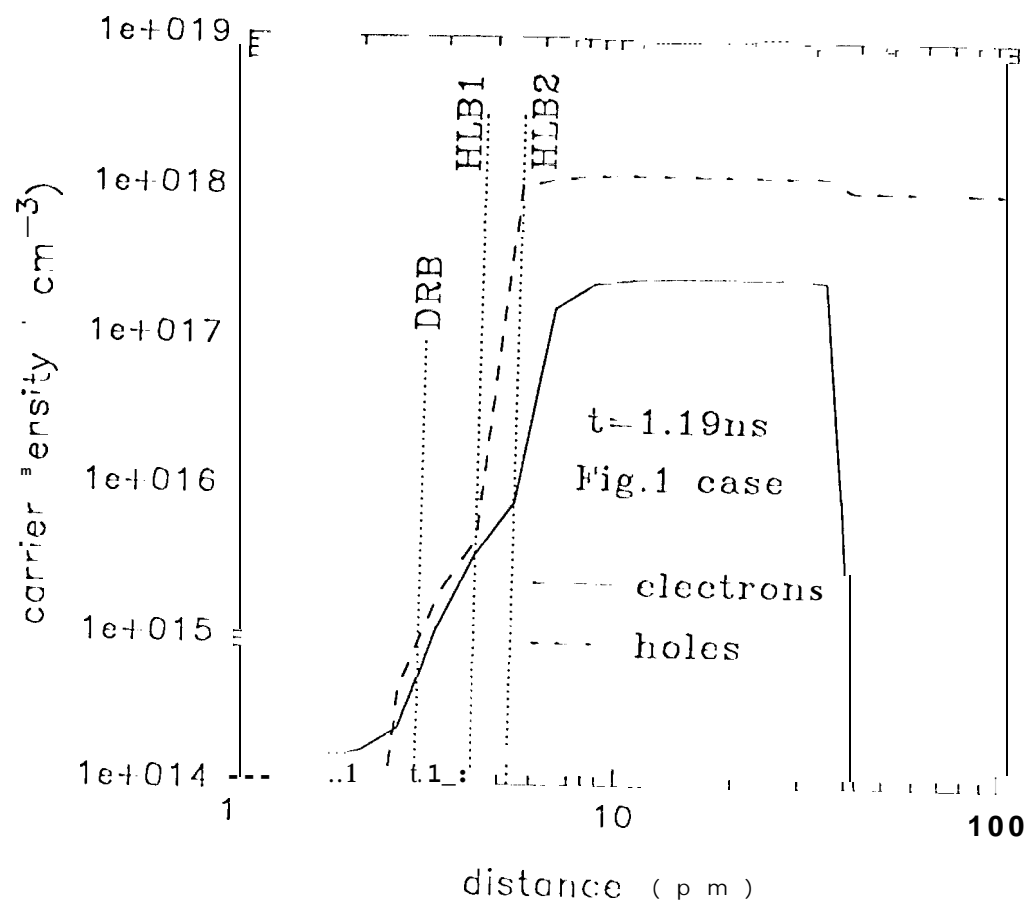


Figure 5: Electron and hole densities for the baseline problem at time t_2 shown in Figure 2.

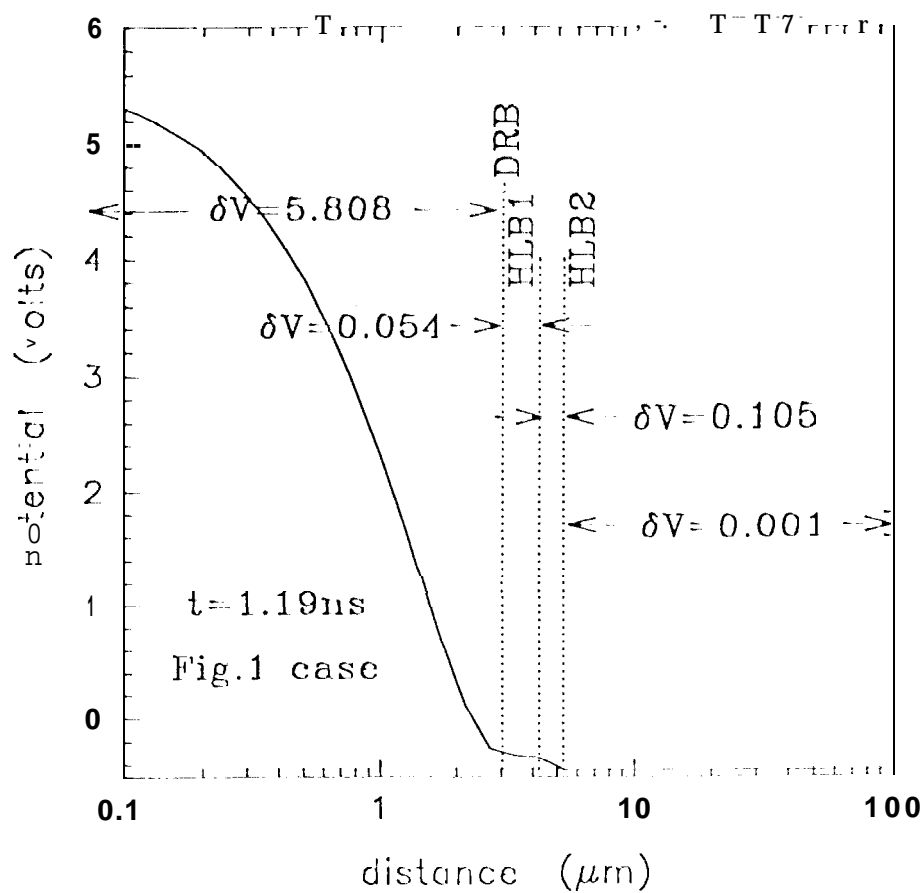


Figure 6: Potential for the baseline problem at time t_2 shown in Figure 2. Off-scale arrow indicates that the first potential difference is across the entire DR.

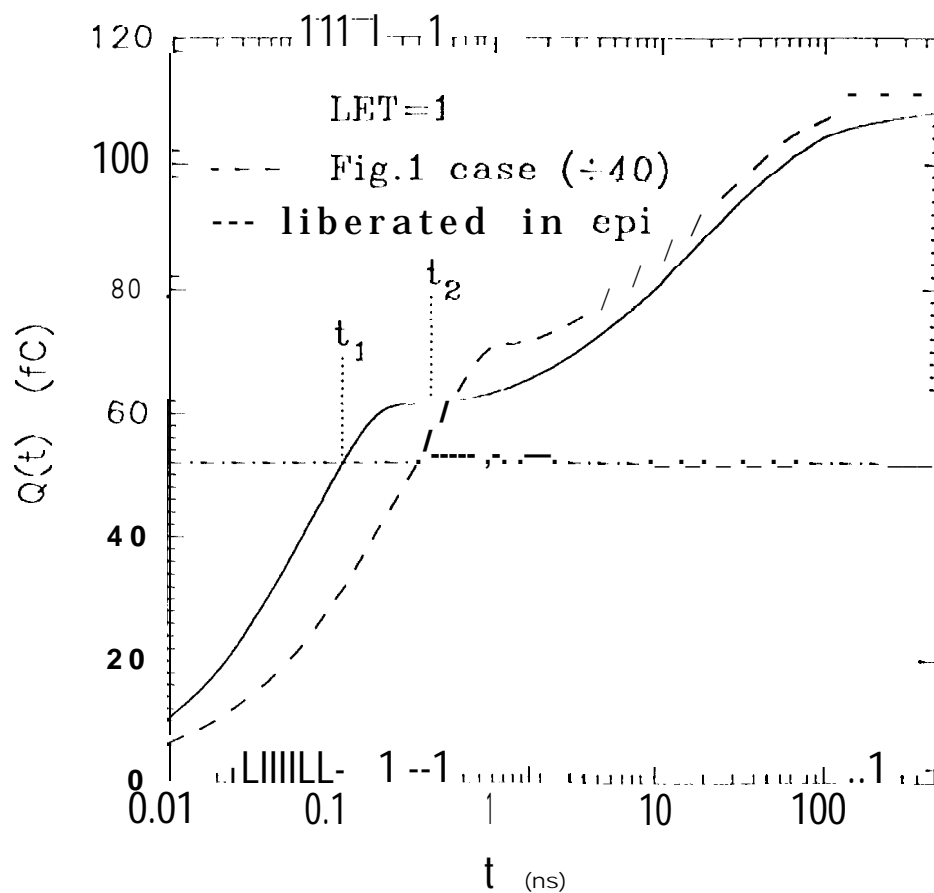


Figure 7 : Collected charge as a function of time for the reduced LET problem. Also shown is the normalized (divided by 40) curve for the baseline case. The horizontal line is the charge liberated in the epi layer.

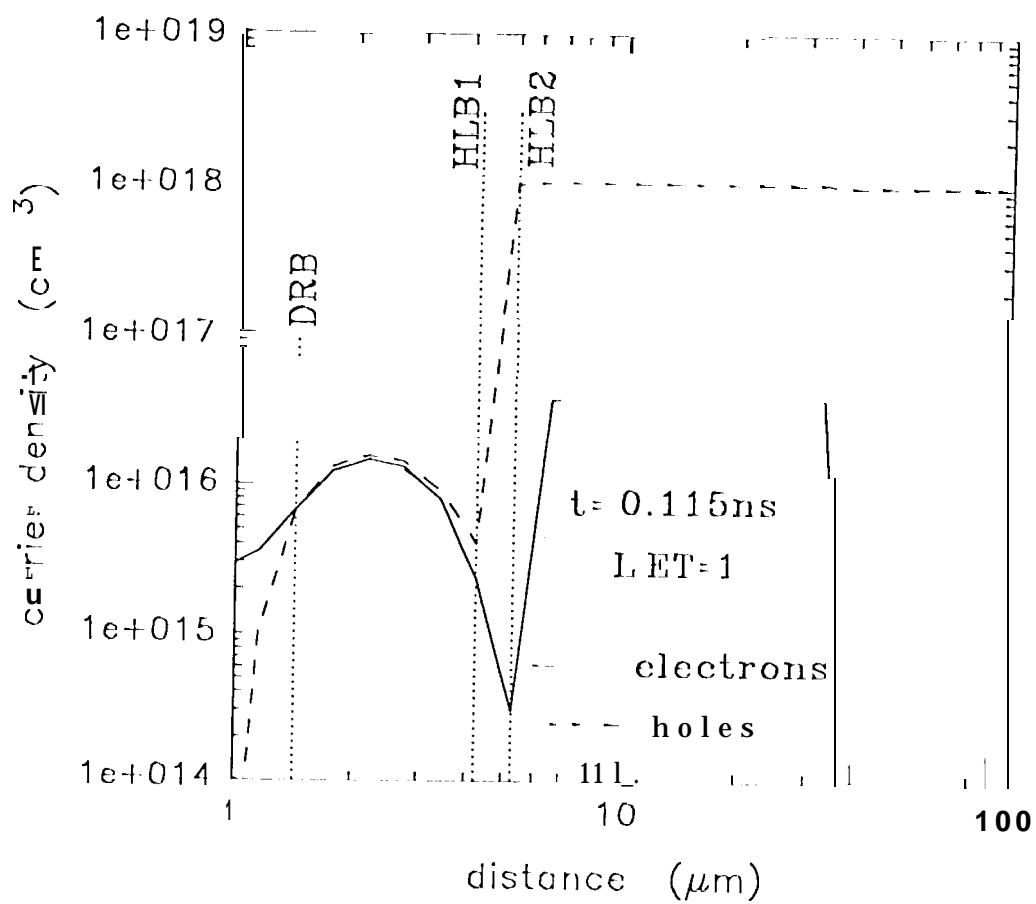


Figure 8: Electron and hole densities for the reduced LET problem at time t_1 shown in Figure 7.

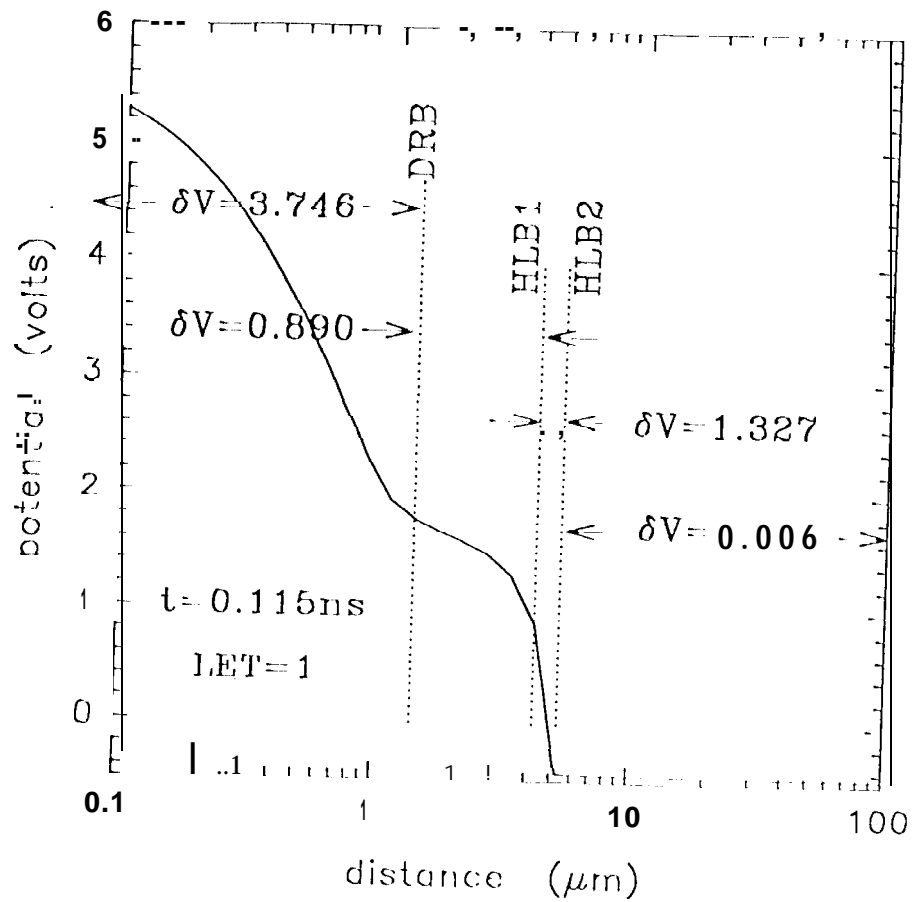


Figure 9: Potential for the reduced LET problem at time t shown in Figure 7. Off-scale arrow indicates that the first potential difference is across the entire DR.

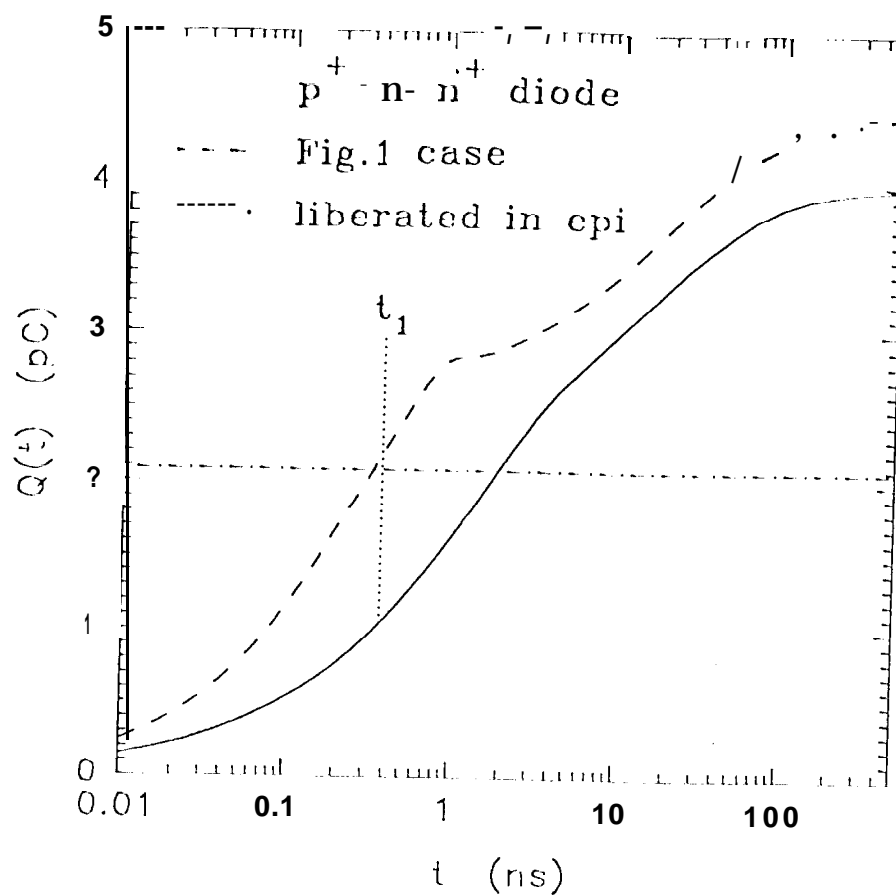


Figure 10: Collected charge as a function of time for the $p^+ - n - n^+$ diode. Also shown is the curve for the baseline case. The horizontal line is the charge liberated in the epi layer.

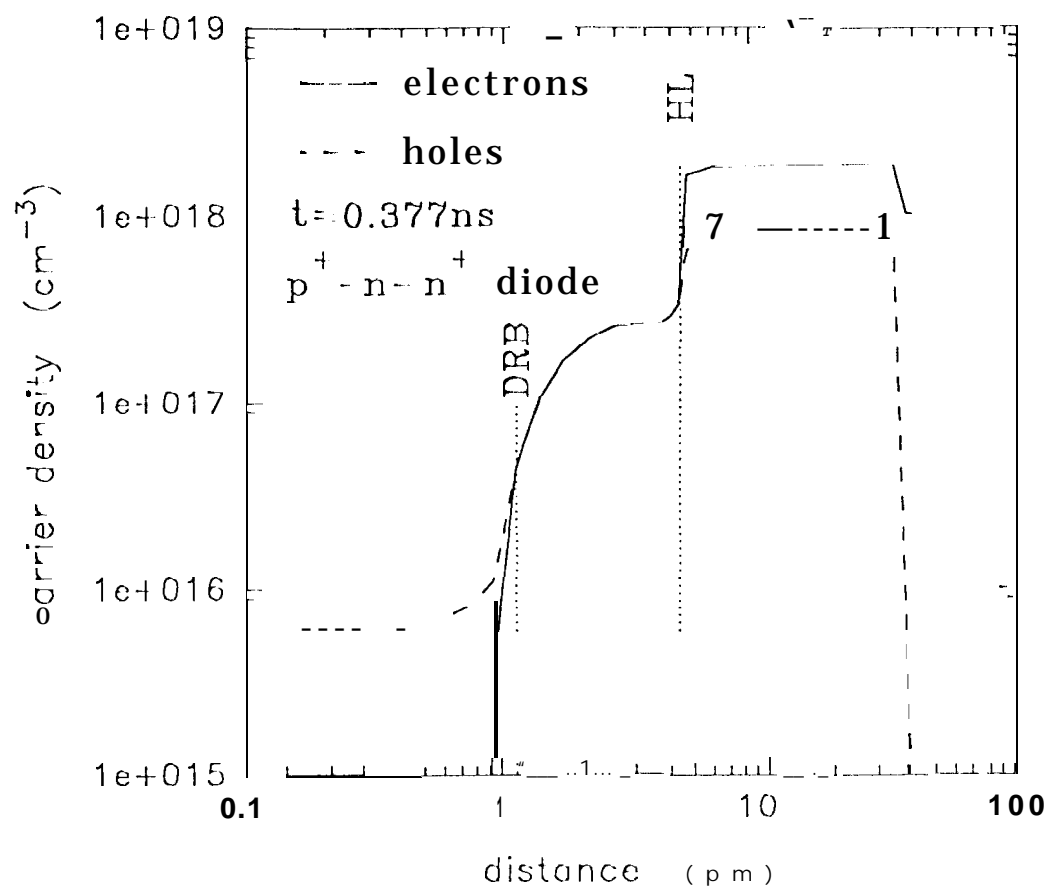


Figure 11: Electron and hole densities for the p⁺-n-n⁺ diode at time t₁ shown in Figure 10.

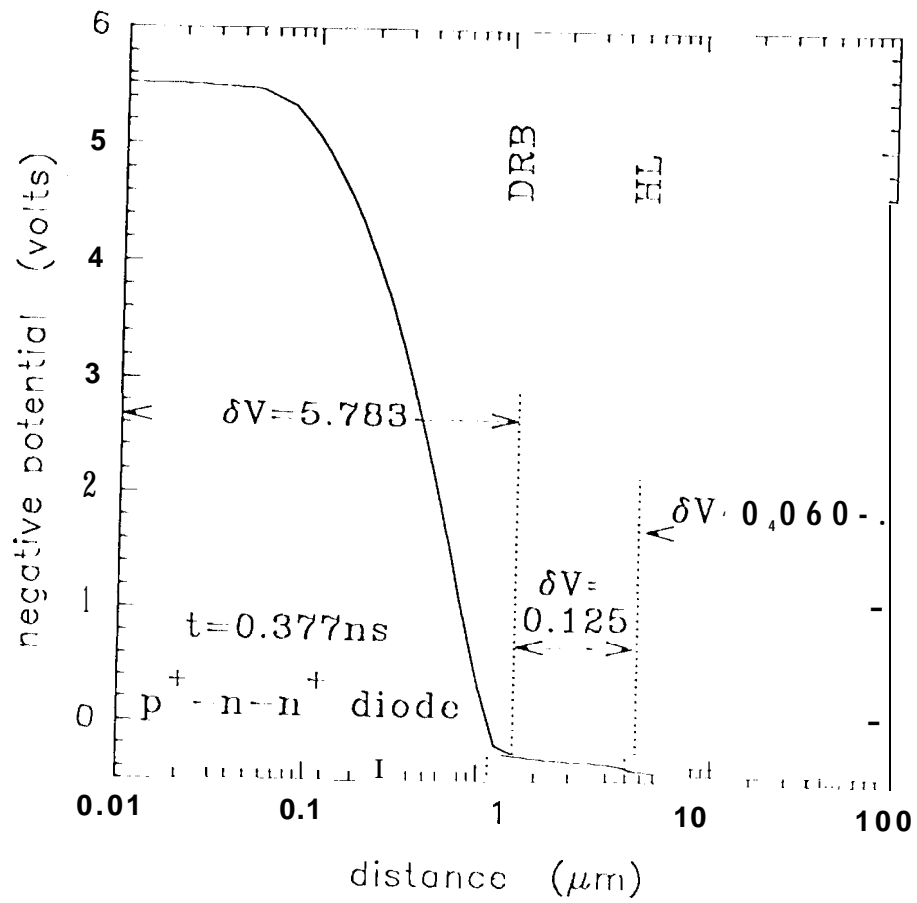


Figure 12: Potential (with reversed sign) for the p^+-n-n^+ diode at time t_1 shown in Figure 1 C1.

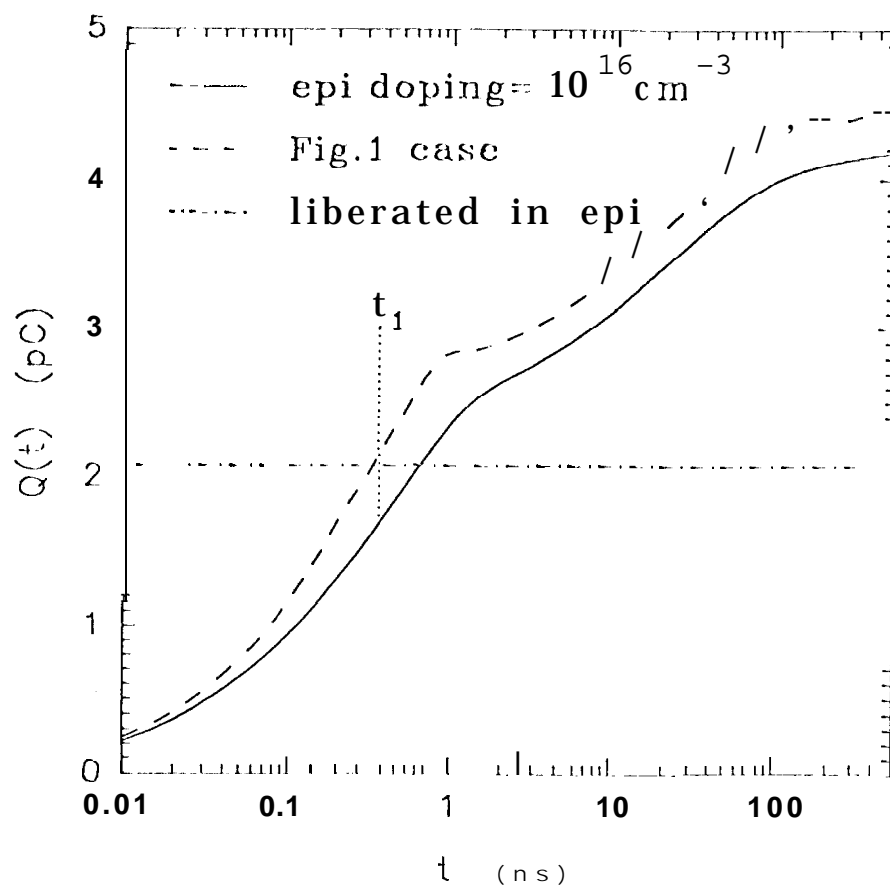


Figure 13: Collected charge as a function of time for the increased epi doping problem. Also shown is the curve for the baseline case. The horizontal line is the charge liberated in the epi layer.

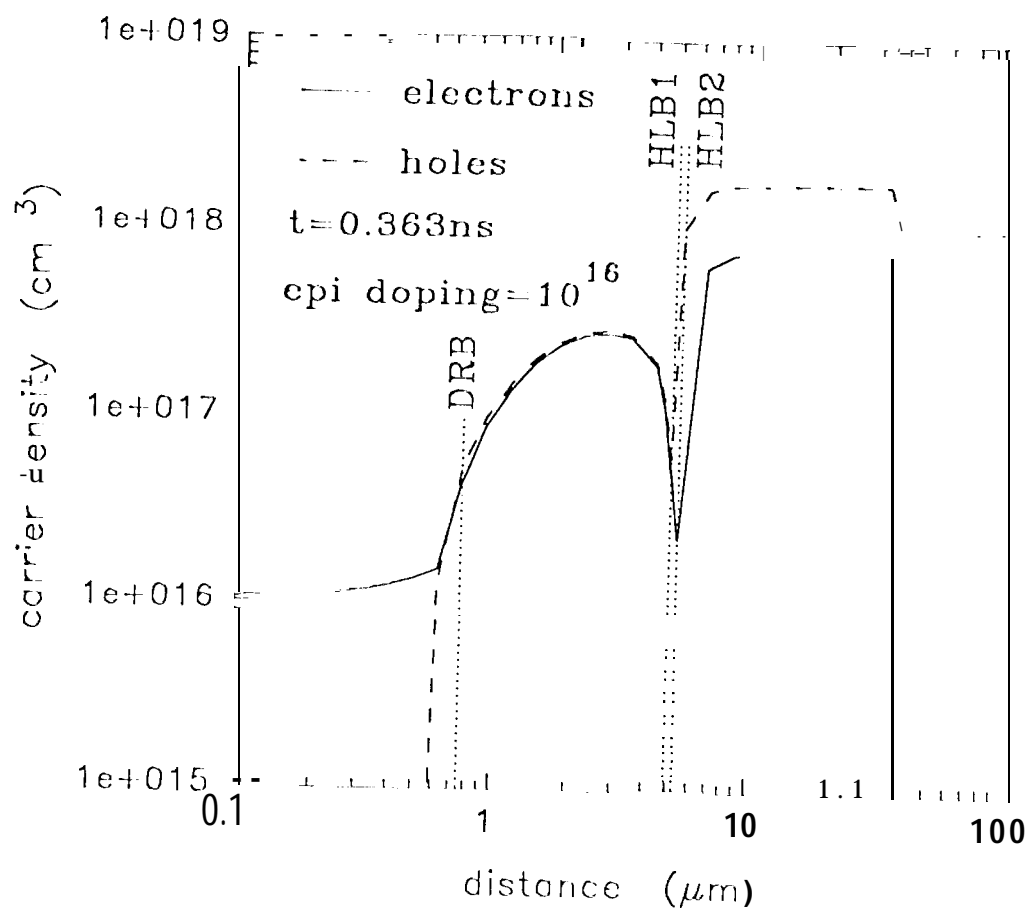


Figure 14: Electron and hole densities for the increased epi doping problem at time t_1 shown in Figure 13.

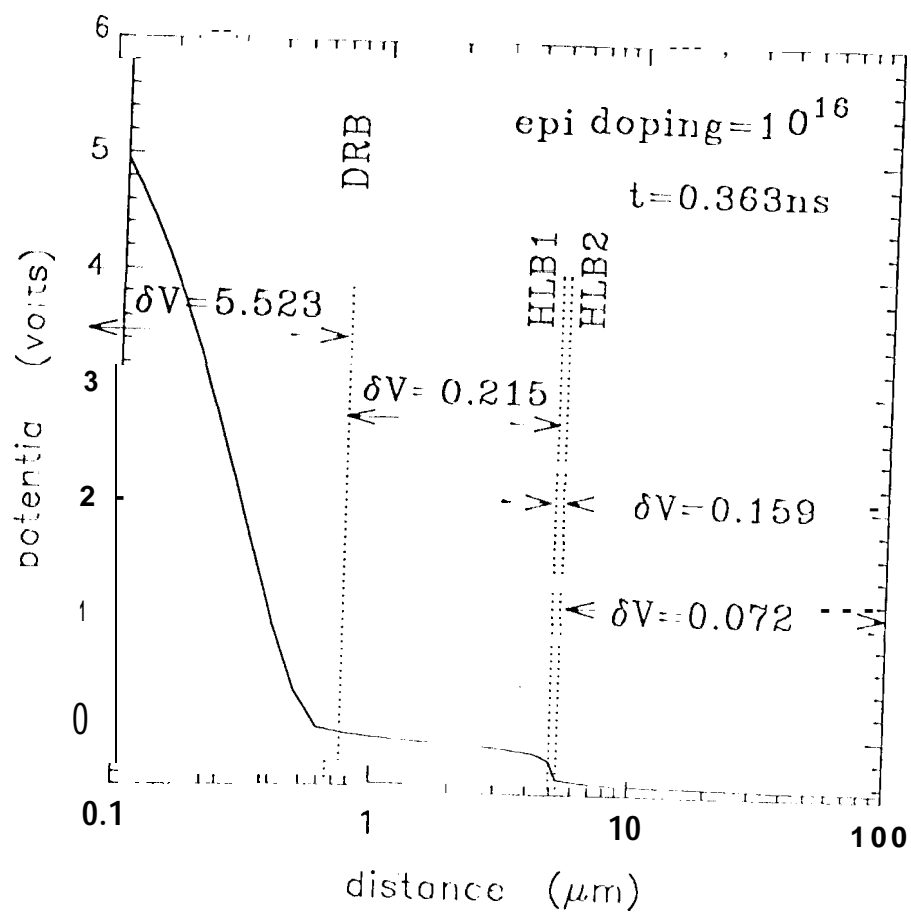


Figure 15: Potential for the increased epi doping problem at time t_1 shown in Figure 33.

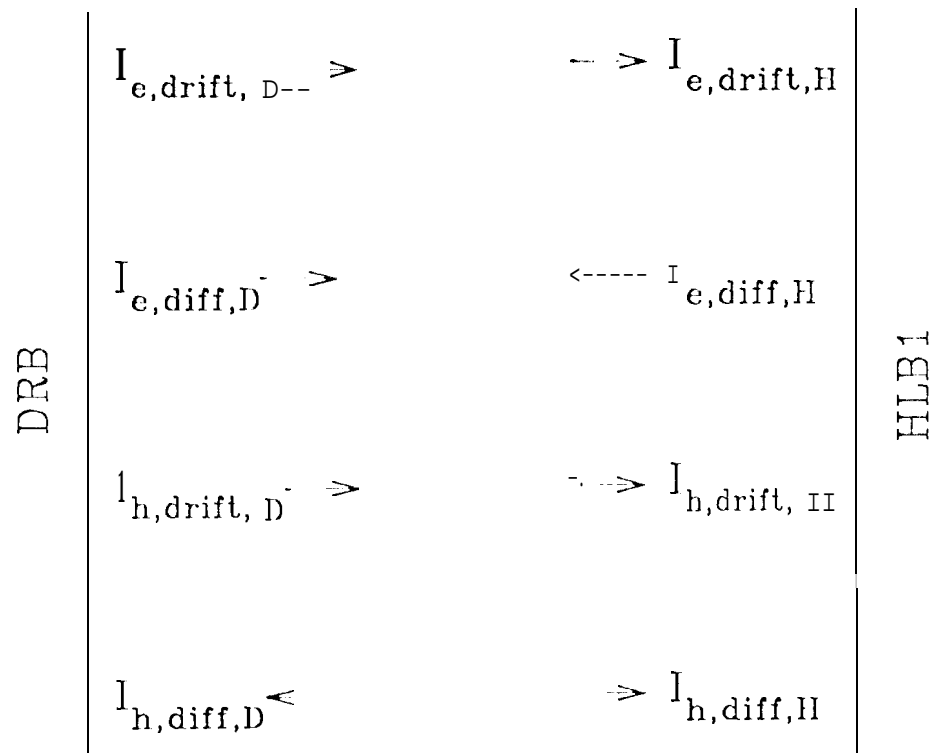


Figure 16: The eight current components at the two quasi-neutral epi region boundaries. Arrows indicate directions that make all components positive for n--p-p⁺ diodes.

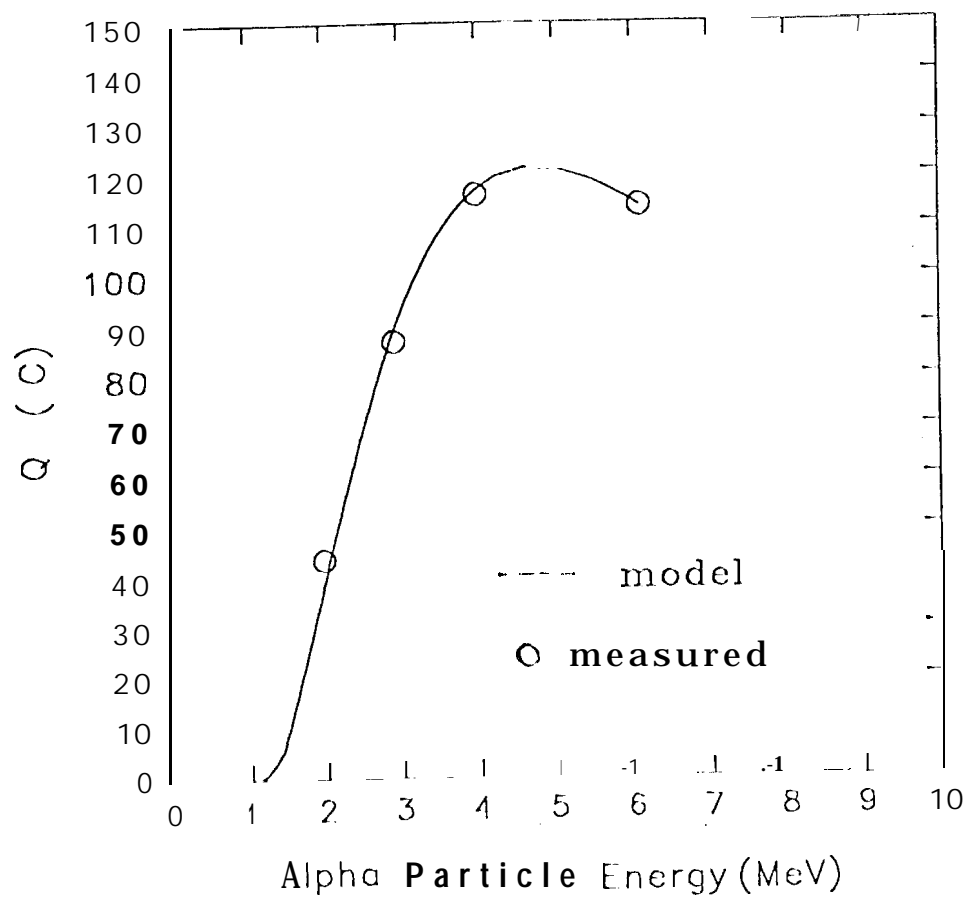


Figure 1.7: Comparison between predicted and measured Q for an epi SRAM .

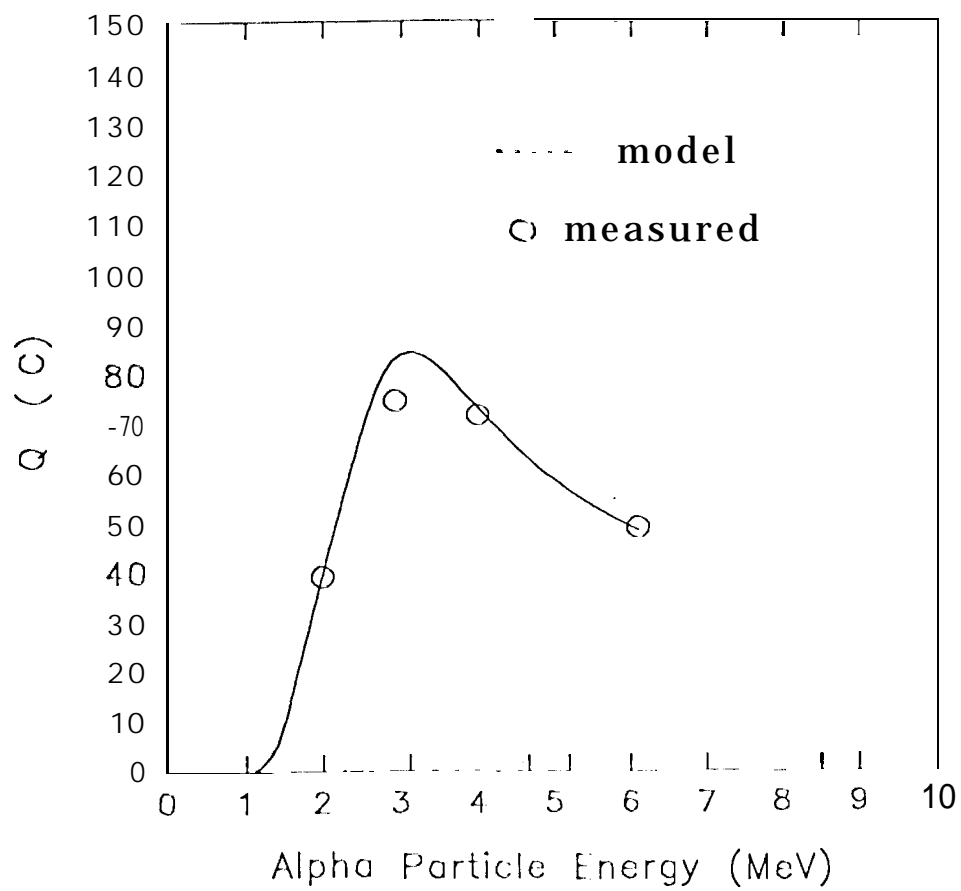


Figure 18: Same as Figure 37 except that the SRAM has a degraded substrate lifetime.